# CFAR Detector for Compressed Sensing Radar Based on $l_1$-norm Minimisation

Dmitrii Kozlov[#1], Peter Ott[#2]
[#]Heilbronn University of Applied Sciences, 74081 Heilbronn, Germany
{[1]dmitrii.kozlov, [2]peter.ott}@hs-heilbronn.de

***Abstract*—Rapidly developing Compressed Sensing theory looks promising for many practical applications, since it allows us to reconstruct K-sparce signals and to reduce some hardware requirements. In this work, we consider the problem of changing noise properties after recovering and its influence on the radar false alarm rate. Due to nonlinearity of the recovering algorithm there is no analytical solution allowing finding a noise distribution after the reconstruction. Therefore, by an empirical approach we come to a solution, where the well-known cell averaging constant false alarm rate detector can be used for a compressed sensing radar. We analyze its performance by simulation and test it with real radar data.**

***Keywords—radar, compressed sensing, detection***

## I. Introduction

The current trend in radars is wider bandwidths. That allows extracting more range information but simultaneously requires faster analog to digital converters (ADCs). Even though modern integrated circuit technology can provide very high conversion rates, the associated power dissipation is often very high [1]. That contrasts with another trend, namely battery powered radars. For example, project Soli is a new sensing technology that uses miniature radar in the form of smartwatch to detect touchless gesture interactions [2]. Radars are used to increase road safety, particularly for animals recognition, and they are powered by solar panels.

Compressed Sensing theory (CS) has been rapidly developed over the last ten years. Beginning from the recovering of purely sparse signals it has come to effective approximation of non-sparse, but compressible, signals [3]. In order to meet the requirements of the above trends one can use ADCs based on CS [4, 5]. The average sample rate can be reduced by more than a magnitude in comparison with the Nyquist rate, e.g. [4] allows digitizing an 800 MHz to 2 GHz band (having 100 MHz of non-contiguous spectral content) at an average sample rate of 236 Msps.

In order to acquire more velocity information radars need smaller pulse repetition time in case of pulse-Doppler radar or shorter ramps in case of frequency modulated continuous wave (FMCW) radar. Reducing these parameters is restricted by hardware limits and other radar operational parameters. By placing pulses or ramps non-uniformly and using CS one can extract more information from a wider velocity range [6].

CS allows us to recover signals of length $N$ from $M \ll N$ measurements at the price of additional calculations. However, the noise distribution is not invariant to the recovering procedure. Due to nonlinearity of recovering algorithms there is no analytical solution allowing finding the noise distribution after recovering. It complicates the use of CS in radar applications, since constant false alarm rate (CFAR) algorithms require knowledge of the noise distribution. There exist two architectures for solving this problem: tuning parameters of the recovering algorithm based on some noise estimation and the standard, non-CS radar approach [7, 8]. In this work, we propose an empirical solution for the second architecture, i.e. firstly we recover the signal by $\ell_1$-norm minimization, secondly estimate noise and detect.

The work is organized as follows. In Section II we describe basics of CS and the reason of noise redistribution. In Section III we describe a process of collecting set of noise samples. In Section IV we show results of fitting known distributions and build a CFAR detector based on one of them. In Section V we build a CFAR detector using maximum likelihood estimation (MLE) of the threshold based on the empirical distribution. In Section VI we test the CFAR detector built in Section IV with real radar signals.

## II. CS Basics

The acquisition of a signal spectrum $\mathbf{x} \in \mathbb{C}^N$ could be represented as

$$\mathbf{y} = \mathbf{\Phi x},$$

where $\mathbf{y} \in \mathbb{C}^M$ is a vector of time measurements, $\mathbf{\Phi}$ is an $M \times N$ matrix that models the measurements system [9]. In case $M = N$, $\mathbf{\Phi}$ represents the inverse discrete Fourier transform (DFT) matrix, that corresponds to the traditional acquisition process with equidistant time measurements.

If $\mathbf{x}$ is $S$-sparse, i.e. it has only $S$ nonzero entries, CS framework allows us to recover $\mathbf{x}$ even when $M \ll N$. The recovery is exact if $M = O(S \log(N/S))$, and time samples are distributed uniformly at random [3].

In real world, measurements contain noise $\mathbf{e} \in \mathbb{C}^M$, $\|\mathbf{e}\|_2 \leq \epsilon$

$$\mathbf{y} = \mathbf{\Phi x} + \mathbf{e}. \tag{1}$$

Moreover, real world signals cannot be purely sparse. However, CS can be used also for the class of compressible signals. We say that $\mathbf{x}$ is compressible if its entries obey a power law

$$|\mathrm{x}|_{(k)} \leq C_r \cdot k^{-r},$$

where $|\mathrm{x}|_{(k)}$ is the $k$th largest value of $\mathbf{x}$ ($|\mathrm{x}|_{(1)} \geq |\mathrm{x}|_{(2)} \geq \cdots \geq |\mathrm{x}|_{(N)}$), $r > 1$, and $C_r$ is a constant which depends only on $r$. In other words, if the sorted magnitudes of $\mathbf{x}$ decay rapidly to zero, the signal is compressible. In such a case with $M$ measurements only, CS stably recovers the $S$-largest entries of $\mathbf{x}$ almost as good as that one would obtain by knowing everything about the signal $\mathbf{x}$ and selecting its $S$-largest entries. [10]

There are a number of algorithms for sparse recovering [11]. Such a variety of algorithms allows us to find a trade-off between computational complexity and goodness of recovery. One of the most successful recovery algorithms is based on $\ell_1$-norm minimization [11, 12]

$$\min \|\hat{\mathbf{x}}\|_1 \quad \text{s. t.} \quad \|\mathbf{\Phi}\hat{\mathbf{x}} - \mathbf{y}\|_2 \leq \epsilon, \tag{2}$$

where $\hat{\mathbf{x}}$ is a recovered vector. Though in contrast to greedy iterative algorithms this approach is computationally expensive, we consider the noise redistribution for this algorithm for two reasons: in some radar applications the problem of computational complexity due to large scale may not arise as often as, for example, in image processing, and goodness of recovery may be important for the detection and measurement process.

When the noise power, which is characterized by parameter $\epsilon$ in (2), is known, the noisy case can be reduced to the sparse case by the constraints in (2). Thus, the signal can be reconstructed exactly up to the amplitude error induced by noise with high probability.

If $\epsilon$ is not known in advance there exist three situations:

- $\epsilon$ is overestimated, i.e. the upper limit of noise power is chosen to calculate this parameter. As a result one "losses" amplitude due to the reconstruction error .
- $\epsilon$ is exact. This is the best case, which corresponds to the optimal reconstruction.
- $\epsilon$ is set less than actual value. In such a case noise can be incorrectly reconstructed as a sparse signal, though noise is not sparse by its nature (white noise is meant here).

## III. Empirical Distribution

In order to get an empirical distribution of noise we use the measurements model (1), where we fix matrix $\mathbf{\Phi}$ once M rows have been chosen uniformly at random from the DFT matrix. The measurement noise values are *i. i. d.* Gaussian, i.e. $\mathbf{e} \sim N(0, \sigma)$. The signal $\mathbf{x}$ is generated, randomly sampled and then reconstructed solving (2) by the log-barrier method. Then the noise values are extracted by removing pure signal components and their neighborhood to minimize the signal influence on noise statistic. The process is repeated for the same $\mathbf{x}$ to collect a noise sample of particular length.

In order to define a threshold the noise samples for different signal to noise ratios and different signal sparsity have to be collected. Further results presented in this work have been achieved by simulations over two fixed sets of noise samples obtained by the described procedure with the initial parameters presented in Table I. One set is used to estimate the distribution and called training set. Another set is used to test built algorithms.

TABLE I. INITIAL PARAMETERS FOR NOISE SET GENERATOR

| Parameter | Value |
|---|---|
| Number of spectrum samples $N$ | 128 |
| Number of time measurements $M$ | 51 |
| Length of a noise samples | $4 \cdot 10^6$ |
| Signal to noise ratios range | 0..10 dB |
| Sparsity levels of signals to be reconstructed, i.e. the ratio between number of tones to be reconstructed and number of time measurements $M$ | $[0.05, 0.1 \ldots, 0.4]$ |

## IV. Fitting Known Distributions

The detection process consists in comparing squared magnitude of $\hat{\mathbf{x}}$ with a threshold. The first attempt to stabilize the false alarm rate is to fit a heavy-tailed distribution. As a criteria of the effectiveness we choose the probability of false alarm $F$. The known and well-studied goodness of fit tests are not proper for that, because these tests exhibit poor sensitivity to deviations from the hypothesized distribution that occur in the tails [13, 14].

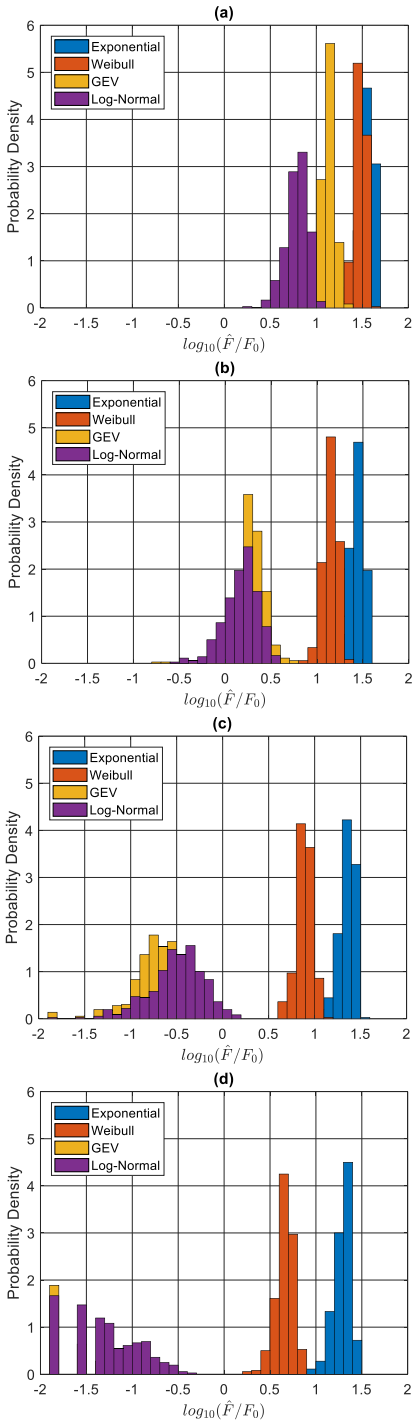


Fig. 1. Relative deviation from desired $F_0 = 10^{-3}$. Labels (a), (b), (c) and (d) correspond to windows of length 10, 20, 40 and 100 respectively.

The results of fitting the Weibull, log-normal, generalized extreme value (GEV) distributions are represented in Fig. 1. It shows the density histograms of the log-ratio between the measured false alarm probability $\hat{F}$ and the desired one $F_0$. The exponential distribution exhibits effectiveness of the

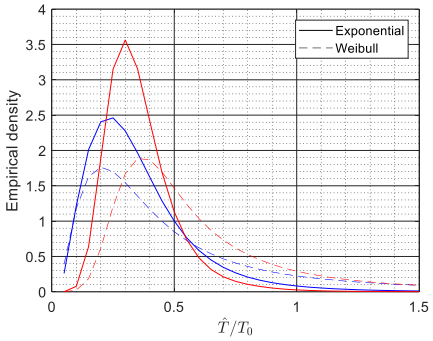


Fig. 2. Probability densities of the threshold errors for window of length 10 (blue) and window of length 40 (red). Each line style corresponds to a different distribution, as indicated in the legend. $F_0 = 10^{-3}$.

standard cell averaging algorithm. Other distributions were also tested but demonstrated poorer results.

Comparing results for windows of length 10 and 20 one can notice that all of the distributions underestimate threshold (most of the $\hat{F}$ errors lies higher than 0, which corresponds to exact estimation). The best results are provided by the log-normal distribution. Further enlarging of window leads to overestimation of the threshold by the log-normal and GEV distributions. Moreover, the log-normal and GEV distributions demonstrate less stable results while increasing relative sparsity, i.e. number of targets.

Though the exponential and Weibull distributions show weaker results, the degree of underestimation is quite stable over wide range of conditions. It gives an idea to compensate the offset using empirical data.

In order to decide between these two distributions we take a closer look at the densities of the threshold errors (ratio between measured threshold $\hat{T}$ and the desired one $T_0$), which are represented in Fig. 2. One can notice two points:

*1) Fitting the exponential distribution provides smaller deviation of the threshold error around the mode than fitting the Weibull distribution.*

*2) The deviation is decreasing while increasing window length. This effect is more noticeable for the exponential distribution.*

These points show us that the use of the exponential distribution with fixed compensation factor is preferred.

Thus, the modified CFAR (MCFAR) detector is reduced to the well-known cell averaging detector with a compensation factor. The compensation factor $k_0$ is chosen as a mode of the ratio $\hat{T}/T_0$ for particular window length. The threshold is given

$$T = -\frac{\ln(F_0)}{k_0 \cdot w} \sum_{i=1}^{w} \hat{\mathbf{x}}_i,$$

where $w$ is a window length.

From a practical point of view MCFAR detector is not new or modified, since for various reasons one already increases threshold by some factor. With this term we just stress the fact that the threshold changes by using CS. In particular, under conditions shown in Section III the threshold increases compared to using whole measurement set ($M = N$).

The results for MCFAR detector represented in Table II show that it stabilizes the false alarm rate. We use here the mode of the threshold estimation error because the mean is influenced by outliers, which can be eliminated by a hit processor.

TABLE II. MODE OF THE THRESHOLD ESTIMATION ERROR AND DEVIATION AROUND IT FOR MCFAR. $F_0 = 10^{-3}$.

| $w$ | 10 | 20 | 40 | 100 |
|---|---|---|---|---|
| $\hat{T}/T_0$ mode | 0.825 | 0.825 | 0.875 | 0.925 |
| Deviation around mode | 4.931 | 3.147 | 2.586 | 2.006 |

## V. MAXIMUM LIKELIHOOD ESTIMATION BASED ON EMPIRICAL DISTRIBUTION

In order to verify the MCFAR detector we build a maximum likelihood estimator (MLE) of the threshold based on an empirical distribution.

| $\mathbf{Threshold}_1$ | $\mathbf{Threshold}_2$ | ⋯ | $\mathbf{Threshold}_K$ |
|---|---|---|---|
| $\mathbf{freqDens}_1{}^1$ | $\mathbf{freqDens}_1{}^2$ | ⋯ | $\mathbf{freqDens}_1{}^K$ |
| $\mathbf{freqDens}_2{}^1$ | $\mathbf{freqDens}_2{}^2$ | ⋯ | $\mathbf{freqDens}_2{}^K$ |
| ⋮ | ⋮ | ⋱ | ⋮ |
| $\mathbf{freqDens}_P{}^1$ | $\mathbf{freqDens}_P{}^2$ | ⋯ | $\mathbf{freqDens}_P{}^K$ |

Fig. 3. LUT for MLE that uses an empirical distribution of the threshold. $P$ is a number of bins, $K$ is a number of threshold estimations, $\mathbf{freqDens}_i{}^j$ is a frequency density of $i$-th bin and $j$-th threshold.

The threshold can be defined as a value of the empirical inverse cumulative distribution function at point $1 - F_0$. Using the training set, we find a vector $\mathbf{Threshold}$ of such values.

From the point of view of MLE the threshold is an unknown parameter of the probability density function (pdf). Pdf for the particular threshold is approximated by a histogram of the sample from the training set. In such a way we build a look up table (LUT) that is schematically shown in Fig. 3.

The threshold is estimated by calculating the likelihood for each column and choosing the value that corresponds to the maximum likelihood. The results of simulation are shown in Fig. 4. The CFAR algorithm based on the empirical distribution has higher computational complexity in contrast to the MCFAR detector, but demonstrates similar results.

## VI. REAL DATA TEST

For the test with real signals, we have used 120 GHz FMCW radar from Silicon Radar®. Input time signal is decimated by the same random pattern as used in Section III, and then reconstructed by $\ell_1$-norm minimisation (Fig. 6). Then original and reconstructed range profiles are compared under different sparsity levels. Radar settings and scene parameters are shown in Table III.

For comparing we use the ratio of the estimated $\hat{F}$ to the desired $F_0$, i.e. $\hat{F}/F_0$, evaluated under different conditions.

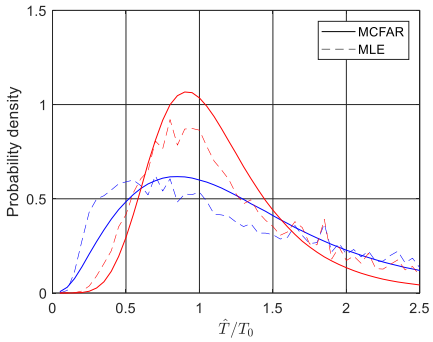


Fig. 4. Probability densities of the threshold errors of MCFAR and MLE for window of length 10 (blue) and window of length 40 (red). $F_0 = 10^{-3}$.

The geometric means and geometric standard deviations of $\hat{F}/F_0$ for windows of length 10 and 20 are shown in Table IV.

TABLE III. RADAR SETTINGS AND SCENE PARAMETERS USED FOR EXPERIMENTAL EVALUATION

| Parameter | Value |
|---|---|
| Base frequency | 119.300 GHz |
| Bandwidth | 3 GHz |
| Sampling rate | 371 kS/s, 117 kS/s |
| Number of targets | {0, 1, 2, 3, 4} |
| Resulting sparsity (taking into account the wide of the target main lobe) | from 0.08 to 0.49 |

TABLE IV. GEOMETRIC MEANS AND STANDARD DEVIATIONS OF THRESHOLD ERRORS FOR REFERENCE MEASUREMENTS AND RECONSTRUCTED ONES, $F_0 = 10^{-3}$

| | *w* | 10 | 20 |
|---|---|---|---|
| G. mean | Reference | 1 | 1.07 |
| | Reconstructed | 0.95 | 0.75 |
| G. std | Reference | 5 | 6.81 |
| | Reconstructed | 2.06 | 2.11 |

The standard deviations show that using MCFAR for reconstructed signal conduces more stable results in contrast to non-CS approach that may seem counterintuitive. The reason consists in a long tailed distribution of noise after reconstruction and the price for that is increase in the threshold in average. The latter can be observed from Fig. 5, which represents probability density function of the ratio between the estimated thresholds for reconstructed measurements $T_{rec}$ and for reference ones $T_{ref}$. Threshold is averaged over each measurement. Thus, it shows the threshold increase in case of using CS instead of complete time measurements.

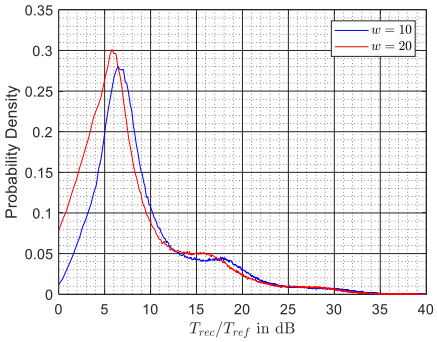


Fig. 5. Threshold increase caused by using recovered signal instead of complete time measurement.

Fig. 7 exhibits the signals of two target scenes reconstructed using $\ell_1$-norm minimisation and the reference ones. The second scene comprises two targets more. Signal to noise ratios at the output of FFT for the targets T1, T2, T3 and T4 are 32.5, 27.5, 18 and 9.3 dB respectively.

Fig. 8 shows Receiver Operating Characteristics (ROC), i.e. probability of detection $D$ against probability of false alarm $F_0$, for both scenes (except for target T4). They reflect the influence of the sparsity level and the previously mentioned threshold increase on detector performance. For each target the ROC curves are shown using windows of length 10 and 20. The ROC curves corresponding to the target detection in a full time signal by the cell averaging CFAR (CA-CFAR) (solid and dash-dot lines in Fig. 8) are close to $D = 1$ and therefore hardly distinguishable. Except for a weaker target T3 (black solid and black dash-dot lines in Fig. 8 (b)).

One can observe that increasing window leads to increasing detector performance. It agrees with simulation results and with practice of non-CS radar. Furthermore, in agreement with CS theory less number of targets guarantees better reconstruction performance and, consequently, might lead to better detection performance. One can notice that comparing ROC curves for targets T1 and T2 in both scenes.

## ACKNOWLEDGMENT

This work was supported by the Ministry for Science, Research and Arts Baden-Württemberg within the project ZAFH MikroSens.

## VII. CONCLUSION

In this work, we demonstrated that noise distribution is significantly changed after signal reconstruction by $\ell_1$-norm

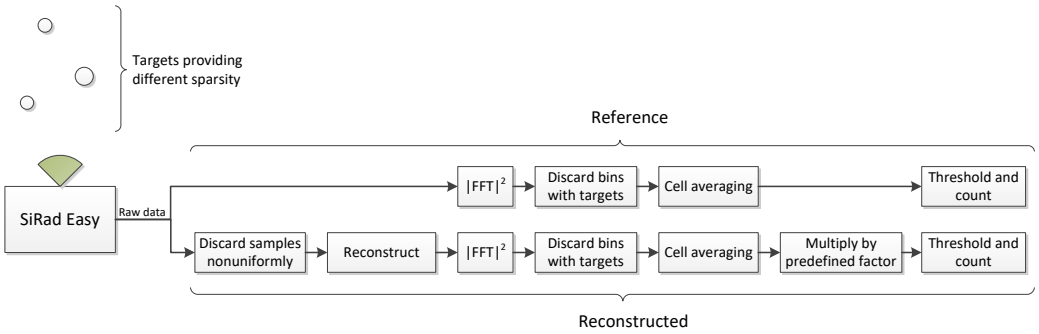


Fig. 6. Experiment chain. "Reference" branch – for complete time signal. "Reconstructed" branch – for time signal sampled uniformly at random.

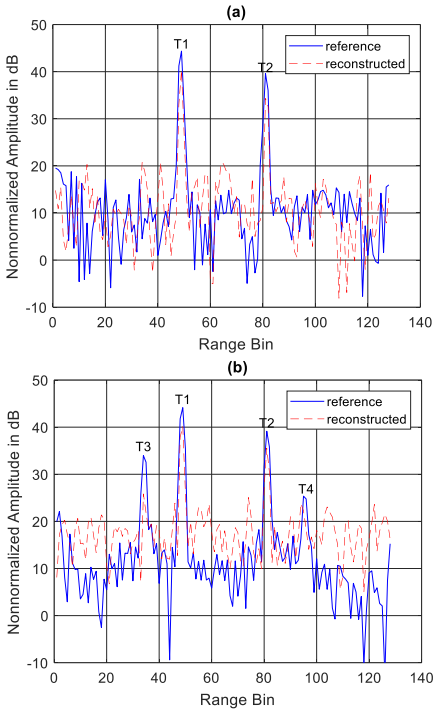


Fig. 7. Range profiles got using full signal and ones got reconstructing by CS for the scene with 2 targets (a) and one with 4 targets (b).

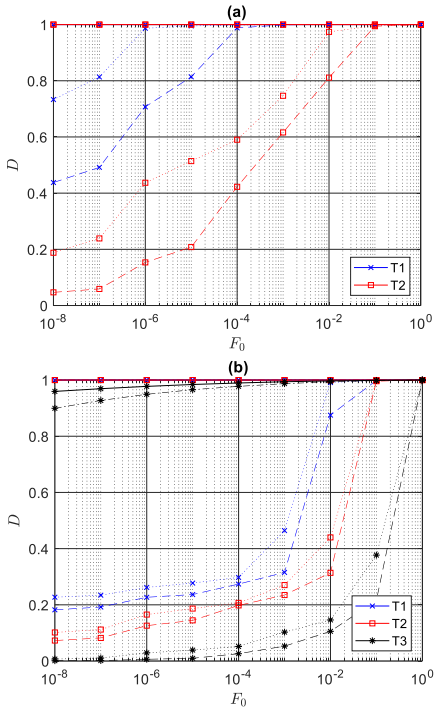


Fig. 8. ROC curves for the scene with 2 targets (a) and one with 4 targets (b). Each colour corresponds to a different target (T1, T2 and T3 in Fig. 7), as indicated in the legend. Each line style corresponds to a combination of a detector and a window length: CA-CFAR, $w = 10$ (solid); CA-CFAR, $w = 20$ (dash-dot); MCFAR, $w = 10$ (dashed); MCFAR, $w = 20$ (dotted).

minimisation. The known distributions are not fitted properly for the false alarm stabilization purpose.

We have proposed the empirical approach to solving this problem. Particularly, by Monte Carlo simulation we have shown that a CA-CFAR algorithm with a threshold increased by a fixed factor can be used for stabilizing false alarm rate in radar compressed sensing application, at least under the specified conditions. We call the algorithm modified in order to underscore that it works with non-exponentially distributed values, as it would be in case of Gaussian noise. However, from an implementation point of view it is usual CA-CFAR algorithm. It has been demonstrated that the modified CFAR produces results close to optimal. By optimal we intend here the results produced by a CFAR algorithm based on real distribution.

The proposed algorithm has been tested with real radar data. Though noise values are not completely *i. i. d.* Gaussian, the results confirm the effectiveness of the method. The price of using CS consists in the threshold increase, i.e. targets have to be stronger to be detected.

## REFERENCES


[1] B. Murmann: "Trends in low-power, digitally assisted A/D conversion," in IEICE Transactions on Electronics, vol. 6, 2010, pp. 718–727.

[2] J. Lien, N. Gillian, M. E. Karagozler, P. Amihood, C. Schwesig, E. Olson, H. Raja, I. Poupyrev, "Soli: ubiquitous gesture sensing with millimeter wave radar," in ACM Transactions on Graphics (TOG), vol.35, n.4, 2016

[3] E. J. Candes, M. Wakin, "An introduction to compressive sampling," in IEEE Signal Processing Magazine, vol. 2, 2008, pp. 21–30.

[4] M. Wakin, S. Becker, E. Nakamura, M. Grant, E. Sovero, D. Ching, J. Yoo, J. Romberg, A. Emami-Neyestanak, E. Candes, "A nonuniform sampler for wideband spectrally-sparse environments," in IEEE Journal on Emerging and Selected Topics in Circuits and Systems, vol. 3, 2012, pp. 516–529.

[5] J. Yoo, C. Turnes, E. Nakamura, C. Le, S. Becker, E. Sovero, M. Wakin, M. Grant, J. Romberg, A. Emami-Neyestanak, E. Candes, "A compressed sensing parameter extraction platform for radar pulse signal acquisition," in IEEE Journal on Emerging and Selected Topics in Circuits and Systems, vol. 3, 2012, pp. 626–638.

[6] M. Herman, T. Strohmer, "High-resolution radar via compressed sensing," in IEEE Transactions on Signal Processing, vol. 6, 2009, pp. 2275–2284.

[7] L. Anitori, A. Maleki, M. Otten, R. Baraniuk, "Design and analysis of compressed sensing radar detectors," in IEEE Transactions on Signal Processing, vol. 4, 2013, pp. 813–827.

[8] H. Kim, A. Haimovich, "Design of cfar radars using compressed sensing," in IEEE Radar Conference, 2016.

[9] J. Laska, M. Davenport, R. Baraniuk, "Exact signal recovery from sparsely corrupted measurements through the pursuit of justice," in Conference Record of the Forty-Third Asilomar Conference on Signals, Systems and Computers, Asilomar, 2009, pp. 1556–1560.

[10] E. Candes, J. Romberg, T. Tao, "Stable signal recovery from incomplete and inaccurate measurements," in Communications on Pure and Applied Mathematics, vol. 59.

[11] J. A. Tropp, S. J. Wright, "Computational methods for sparse solution of linear inverse problems," in Proceedings of the IEEE, vol. 6, 2010, pp. 948–958.

[12] A. Maleki, L. Anitori, Z. Yang, R. Baraniuk, "Asymptotic analysis of complex lasso via complex approximate message passing (CAMP)," in IEEE Transactions on Information Theory, vol. 7, 2013, pp. 4290–4308.

[13] D. Mason, J. Schuenemeyer, "A modified Kolmogorov-Smirnov test sensitive to tail alternatives," in The Annals of Statistics, vol. 3, 1983, pp. 933–946.

[14] J. Diebolt, M. Garrido, S. Girard, "A goodness-of-fit test for the distribution tail," in Topics in Extreme Values, M. Ahsanullah and S.N.U.A. Kirmani, Nova Science: NewYork, 2007, pp. 95–109.